Mottness-induced healing in strongly correlated superconductors: supplemental material

Shao Tang,[1] E. Miranda,[2] and V. Dobrosavljevic[1]

[1] *Department of Physics and National High Magnetic Field Laboratory,*
Florida State University, Tallahassee, Florida 32306, USA
[2] *Instituto de Física Gleb Wataghin, Campinas State University,*
Rua Sérgio Buarque de Holanda, 777, CEP 13083-859, Campinas, Brazil

I. THE LINEAR APPROXIMATION

Our linear approximation approach consists of expanding the mean-field equations (2-5) of the main text to first order in the site energies ε_i. Denoting linear deviations in the various fields by δ we get

$$\delta\chi_{ij} = 2kT\sum_{nl}\left(-g_{il}g_{lj}+G_{1il}G_{1lj}\right)\left(\delta\lambda_l+\varepsilon_l\right)+2kTr\sum_{nlm}\left(-g_{il}g_{mj}+G_{1il}G_{1mj}\right)\left(\delta r_l h_{lm}+\delta r_m h_{lm}\right)$$
$$-2kT\sum_{nlm}\left(-g_{il}g_{mj}+G_{1il}G_{1mj}\right)\left(\widetilde{J}\delta\chi_{lm}\right)+2kT\sum_{nlm}\left(g_{il}G_{1mj}+g_{mj}G_{1il}\right)\left(\widetilde{J}\delta\Delta_{lm}\right), \tag{1}$$

$$\delta\Delta_{ij} = -2kT\sum_{nl}\left(g_{il}G_{1lj}+g_{lj}G_{1il}\right)\left(\delta\lambda_l+\varepsilon_l\right)-2kTr\sum_{nlm}\left(g_{il}G_{1mj}+g_{mj}G_{1il}\right)\left(\delta r_l h_{lm}+\delta r_m h_{lm}\right)$$
$$+2kT\sum_{nlm}\left(g_{il}G_{1mj}+g_{mj}G_{1il}\right)\left(\widetilde{J}\delta\chi_{lm}\right)-2kT\sum_{nlm}\left(G_{1il}G_{2mj}+g_{il}g_{mj}\right)\left(\widetilde{J}\delta\Delta_{lm}\right), \tag{2}$$

$$-r\delta r_i = kT\sum_{nl}\left(-g_{il}g_{li}+G_{1il}G_{1li}\right)\left(\delta\lambda_l+\varepsilon_l\right)+kTr\sum_{nlm}\left(-g_{il}g_{mi}+G_{1il}G_{1mi}\right)\left(\delta r_l h_{lm}+\delta r_m h_{lm}\right)$$
$$-kT\sum_{nlm}\left(-g_{il}g_{mi}+G_{1il}G_{1mi}\right)\left(\widetilde{J}\delta\chi_{lm}\right)+kT\sum_{nlm}\left(g_{il}G_{1mi}+g_{mi}G_{1il}\right)\left(\widetilde{J}\delta\Delta_{lm}\right), \tag{3}$$

$$\lambda\delta r_i+r\delta\lambda_i+\sum_l h_{il}\chi_{il}\delta r_l+r\sum_l h_{il}\delta\chi_{il} = 0, \tag{4}$$

where $G_{1ij}\equiv[G_{ij}]_{11}$, $G_{2ij}\equiv[G_{ij}]_{22}$, $g_{ij}\equiv[G_{ij}]_{12}=[G_{ij}]_{21}$ are the Green's functions of the clean system, n is the fermionic Matsubara frequency index and $\widetilde{J}=\frac{3}{8}J$. The latter choice is made, in the presence of correlations, so that the multi-channel Hubbard-Stratonovich transformation we used reproduces, at the saddle-point level, the mean-field results [1][2]. In general, the clean Green's functions in **k**-space are given by

$$G_1(\omega_n,\mathbf{k}) = \frac{i\omega_n+e(\mathbf{k})}{(i\omega_n)^2-e^2(\mathbf{k})-\widetilde{J}^2\Delta^2(\mathbf{k})}, \tag{5}$$

$$G_2(\omega_n,\mathbf{k}) = \frac{i\omega_n-e(\mathbf{k})}{(i\omega_n)^2-e^2(\mathbf{k})-\widetilde{J}^2\Delta^2(\mathbf{k})}, \tag{6}$$

$$g(\omega_n,\mathbf{k}) = \frac{\widetilde{J}\Delta(\mathbf{k})}{(i\omega_n)^2-e^2(\mathbf{k})-\widetilde{J}^2\Delta^2(\mathbf{k})}, \tag{7}$$

where the renormalized dispersion is

$$e(\mathbf{k}) \;=\; -2\left(xt + \chi\widetilde{J}\right)\left[\cos\left(k_x a\right) + \cos\left(k_y a\right)\right] - 4xt'\cos\left(k_x a\right)\cos\left(k_y a\right) - \mu, \tag{8}$$

we have absorbed the clean λ in the chemical potential, and

$$\Delta\left(\mathbf{k}\right) = 2\Delta_0\left[\cos\left(k_x a\right) - \cos\left(k_y a\right)\right]. \tag{9}$$

Notice that the dimensionful gap function is $\Delta_{phys}\left(\mathbf{k}\right) = \widetilde{J}\Delta\left(\mathbf{k}\right)$. As we focus on the asymptotic long-range behavior of the different fields, their variations are dominated by the corresponding clean-limit symmetry channel. We therefore define local order parameters as $\delta\chi_i \equiv \frac{1}{2d}\sum_j \delta\chi_{ij}\Gamma(s)_{ij}$, $\delta\Delta_i \equiv \frac{1}{2d}\sum_j \delta\Delta_{ij}\Gamma(d_{x^2-y^2})_{ij}$. Thus, *defining vectors and matrices in the lattice site basis with bold-face letters*, Eqs. (1-4) can be recast as

$$\left(\boldsymbol{A} + r^2\boldsymbol{B}\right)\delta\boldsymbol{\Phi} = r^2\boldsymbol{C}, \tag{10}$$

where

$$\boldsymbol{A} = \begin{pmatrix} \boldsymbol{M}_{11} & \boldsymbol{M}_{12} & \boldsymbol{M}_{13} & \boldsymbol{M}_{14} \\ \boldsymbol{M}_{21} & \boldsymbol{M}_{22} & \boldsymbol{M}_{23} & \boldsymbol{M}_{24} \\ \boldsymbol{M}_{31} & \boldsymbol{M}_{32} & \boldsymbol{M}_{33} & \boldsymbol{M}_{34} \\ 0 & 0 & \lambda\boldsymbol{1} - \frac{\lambda}{2d}\boldsymbol{\Gamma}(s) & 0 \end{pmatrix}, \boldsymbol{B} = \begin{pmatrix} 0 & 0 & 0 & 0 \\ 0 & 0 & 0 & 0 \\ 0 & 0 & 0 & 0 \\ -2dt\boldsymbol{1} & 0 & 0 & \boldsymbol{1} \end{pmatrix}, \delta\boldsymbol{\Phi} = \begin{pmatrix} \delta\boldsymbol{\chi} \\ \delta\boldsymbol{\Delta} \\ r\delta\boldsymbol{r} \\ \delta\overline{\boldsymbol{\lambda}} \end{pmatrix}, \boldsymbol{C} = \begin{pmatrix} 0 \\ 0 \\ 0 \\ \boldsymbol{\varepsilon} \end{pmatrix}. \tag{11}$$

Here, the elements of (the vector) $\boldsymbol{\varepsilon}$ are the disorder potential values ε_i, $\boldsymbol{1}$ is the identity matrix, $\delta\overline{\lambda}_i = \delta\lambda_i + \varepsilon_i$, and

$$M_{11ij} = -\delta_{ij} - \frac{\widetilde{J}kT}{d}\sum_{nml}\Gamma(s)_{il}\left(-g_{ij}g_{ml} + G_{1ij}G_{1ml}\right)\Gamma(s)_{jm} \tag{12}$$

$$M_{12ij} \;=\; \frac{\widetilde{J}kT}{d}\sum_{nml}\Gamma(s)_{il}\left(g_{ij}G_{1ml} + g_{ml}G_{1ij}\right)\Gamma(d_{x^2-y^2})_{jm} \tag{13}$$

$$M_{13ij} \;=\; \frac{kT}{d}\sum_{nml}\Gamma(s)_{il}\left(-g_{ij}g_{ml} + G_{1ij}G_{1ml} - g_{im}g_{jl} + G_{1im}G_{1jl}\right)h_{jm} \tag{14}$$

$$M_{14ij} = \frac{kT}{d}\sum_{nl}\Gamma(s)_{il}\left(-g_{ij}g_{jl} + G_{1ij}G_{1jl}\right) \tag{15}$$

$$M_{21ij} \;=\; -\frac{\widetilde{J}kT}{d}\sum_{nml}\Gamma(d_{x^2-y^2})_{il}\left(g_{ij}G_{1ml} + g_{ml}G_{1ij}\right)\Gamma(s)_{jm} \tag{16}$$

$$M_{22ij} \;=\; \delta_{ij} + \frac{\widetilde{J}kT}{d}\sum_{nml}\Gamma(d_{x^2-y^2})_{il}\left(G_{1ij}G_{2ml} + g_{ij}g_{ml}\right)\Gamma(d_{x^2-y^2})_{jm} \tag{17}$$

$$M_{23ij} \;=\; \frac{kT}{d}\sum_{nml}\Gamma(d_{x^2-y^2})_{il}\left(g_{ij}G_{1ml} + g_{ml}G_{1ij} + g_{im}G_{1jl} + g_{jl}G_{1im}\right)h_{jm} \tag{18}$$

$$M_{24ij} = \frac{kT}{d}\sum_{nl}\Gamma(d_{x^2-y^2})_{il}\left(g_{ij}G_{1jl} + g_{jl}G_{1ij}\right) \tag{19}$$

$$M_{31ij} = -\widetilde{J}kT \sum_{nm} \left(-g_{ij}g_{mi} + G_{1ij}G_{1mi} \right) \Gamma(s)_{jm} \tag{20}$$

$$M_{32ij} = \widetilde{J}kT \sum_{nm} \left(g_{ij}G_{1mi} + g_{mi}G_{1ij} \right) \Gamma(d_{x^2-y^2})_{jm} \tag{21}$$

$$M_{33ij} = \delta_{ij} + kT \sum_{nm} h_{jm} \left(-g_{ij}g_{mi} + G_{1ij}G_{1mi} - g_{im}g_{ji} + G_{1im}G_{1ji} \right) \tag{22}$$

$$M_{34ij} = kT \sum_{n} \left(-g_{ij}g_{ji} + G_{1ij}G_{1ji} \right) \tag{23}$$

In writing Eqs. (10), we have made explicit the r dependence of Eqs. (1-4). We note, however, that there is also an implicit dependence on r through the dispersion (8) (where $x = r^2$), which enters the various Green's functions in Eqs. (5-7).

Since the matrix elements in Eqs. (12-23) are all calculated in the *translation-invariant clean system*, Eqs. (10) can be easily solved in **k**-space by matrix inversion. Normal state results are obtained by removing the second row and column and setting $\Delta(\mathbf{k})$ to zero. Non-correlated results correspond to the absence of slave bosons and constraints, so we just remove the third and fourth rows and columns and set $x = 1$ and $\lambda_i = 0$. In every case, the clean limit is first solved self-consistently for χ, Δ, λ and μ, and then the fluctuations in the presence of impurities are obtained.

In discussing the solution to Eqs. (10), we rely on the fact that all quantities in Eqs. (12-23) are non-singular and finite as $x \to 0$. Thus, we can write their formal solution as

$$\delta\boldsymbol{\Phi} = r^2 \left(\boldsymbol{A} + r^2\boldsymbol{B} \right)^{-1} \boldsymbol{C} = r^2\boldsymbol{A}^{-1}\boldsymbol{C} + \mathcal{O}\left(r^4 \right). \tag{24}$$

It follows that $\delta\chi_i$, $\delta\Delta_i$, $r\delta r_i$, and $\delta\overline{\lambda}_i = \delta\lambda_i + \varepsilon_i$ are all of order $r^2 = x$.

II. THE GAP FLUCTUATIONS AND THE HEALING FACTOR

In order to characterize quantitatively the healing process in the SC state, we focused on the linear gap response to the disorder potential

$$\delta\Delta_i = \Delta_0 \sum_j M_\Delta \left(\mathbf{r}_i - \mathbf{r}_j \right) \varepsilon_j, \tag{25}$$

which is obtained directly from the second line of the solution to Eqs. (24). In order to gain further insight, we separated the local and non-local parts of the gap response as follows. In Eqs. (10) as defined in real space, we separate sums over sites into a local part, with sums up to next-to-nearest neighbors (denoted by $r_{ij} \leq \sqrt{2}a$), and a non-local part, with sums over the remaining sites (denoted by $r_{ij} > \sqrt{2}a$). For example,

$$\sum_j M_{11ij}\delta\chi_j = \sum_{j,r_{ij} \leq \sqrt{2}a} M_{11ij}\delta\chi_j + \sum_{j,r_{ij} > \sqrt{2}a} M_{11ij}\delta\chi_j, \text{ etc.} \tag{26}$$

After solving the equations, this separation naturally defines local and non-local responses of the various fields. In **k**-space, we can write

$$M_\Delta \left(\mathbf{k} \right) = M_{\Delta,loc} \left(\mathbf{k} \right) + M_{\Delta,nonloc} \left(\mathbf{k} \right). \tag{27}$$

This procedure is equivalent to projecting the full response in **k**-space onto some lattice symmetry channels with different ranges: $\Gamma_s \left(\mathbf{k} \right) = 2\left[\cos\left(k_x a \right) + \cos\left(k_y a \right) \right]$ for nearest neighbors, and so on. Then, the power spectrum of spatial gap fluctuations follows naturally from this separation

$$S\left(\mathbf{k} \right) = M_\Delta^2 \left(\mathbf{k} \right), \tag{28}$$

$$S_{loc}\left(\mathbf{k} \right) = M_{\Delta,loc}^2 \left(\mathbf{k} \right), \tag{29}$$

$$S_{nonloc}\left(\mathbf{k} \right) = \left[M_\Delta \left(\mathbf{k} \right) - M_{\Delta,loc} \left(\mathbf{k} \right) \right]^2. \tag{30}$$
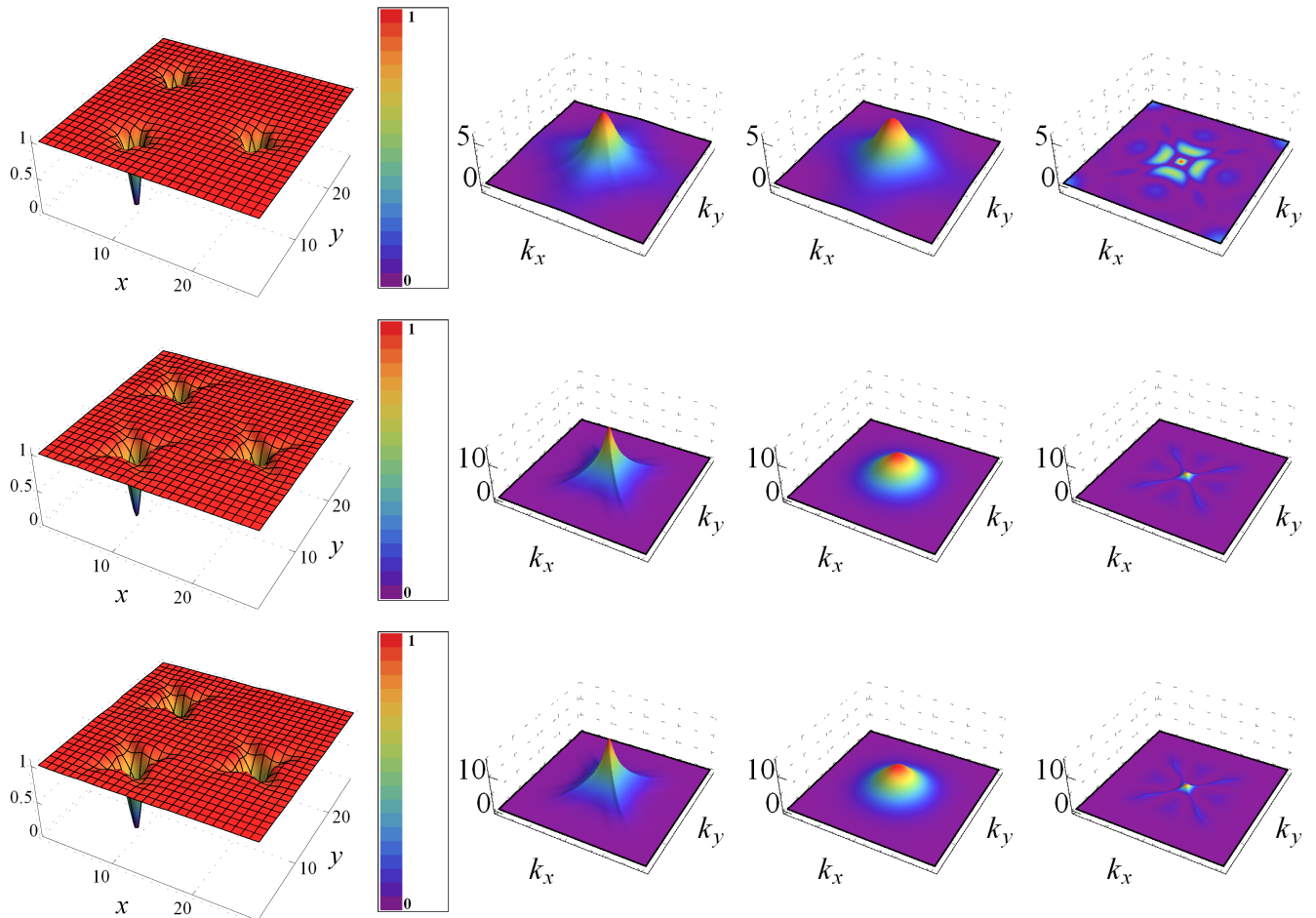
Figure 1: Spatial variations of normalized local gap function $\frac{\delta\Delta_i}{\Delta_0}$ for three impurities (first column) and the corresponding power spectra $S(\mathbf{k})$, $S(\mathbf{k})_{loc}$ and $S(\mathbf{k})_{nonloc}$ (second to fourth columns) for $x = 0.15$ (first row), $x = 0.25$ (second row), and $x = 0.3$ (third row). The corresponding healing factors are (a) $h = 0.23\%$, (b) $h = 1.77\%$, and (c) $h = 2.74\%$.

Finally, we define the healing factor as the ratio of integrated non-local to local contributions to the power spectrum

$$h = \frac{\int S_{nonloc}(\mathbf{k}) \, d^2 k}{\int S_{loc}(\mathbf{k}) \, d^2 k}.$$

(31)

The gap fluctuations $\delta\Delta_i$ for three impurities and power spectra, for several dopings and in the presence of correlations, are shown in Fig. 1. The strong healing in the presence of correlations is conspicuous. It is important to note that this suppression of gap fluctuations is not restricted to small dopings and remains quite strong even at $x = 0.3$, where the healing factor does not exceed 3%. As explained in the main text, the healing effect originates in the dominance of the local spherically symmetric part (third column in Fig. 1) over the anisotropic non-local response (fourth column in Fig. 1).

III. THE IRRELEVANCE OF SPINON FLUCTUATIONS AND THE "MINIMAL MODEL"

We can shed light on the strong healing effect by studying a simplified case obtained by "turning off" the $\delta\chi_i$ fluctuations. In this case, we need to solve the smaller set of equations

$$\begin{pmatrix} \boldsymbol{M}_{22} & \boldsymbol{M}_{23} & \boldsymbol{M}_{24} \\ \boldsymbol{M}_{32} & \boldsymbol{M}_{33} & \boldsymbol{M}_{34} \\ 0 & \lambda\mathbf{1} - \frac{\lambda}{2d}\boldsymbol{\Gamma}(s) & r^2\mathbf{1} \end{pmatrix} \begin{pmatrix} \delta\boldsymbol{\Delta} \\ r\delta\boldsymbol{r} \\ \delta\bar{\boldsymbol{\lambda}} \end{pmatrix} = \begin{pmatrix} 0 \\ 0 \\ r^2\boldsymbol{\varepsilon} \end{pmatrix}.$$

(32)
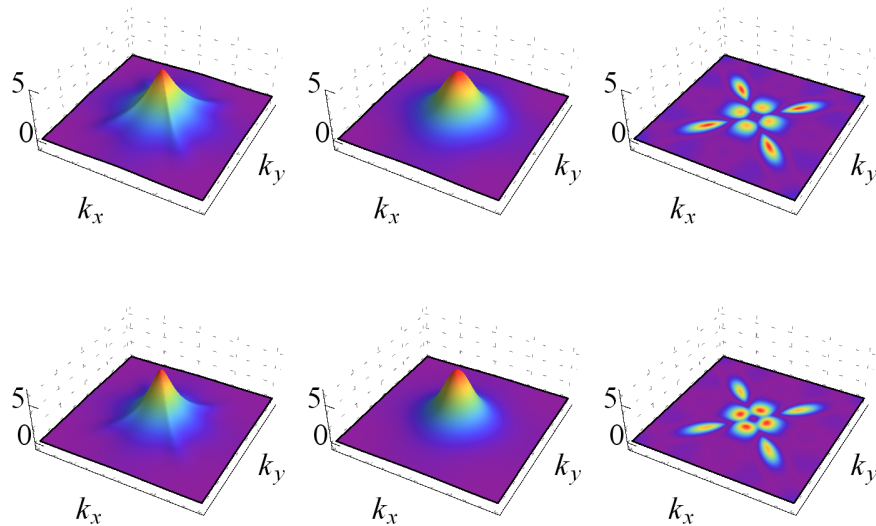
Figure 2: Power spectra of gap fluctuations $S(\mathbf{k})$, $S(\mathbf{k})_{loc}$ and $S(\mathbf{k})_{nonloc}$ (first to third columns) for $x = 0.2$ in the presence of correlations. The top figures were obtained from the full solution of the linearized Eqs. (10), whereas the bottom ones correspond to the minimal model (Eqs. (34)). Note that the healing factors are $h = 0.74\%$ (top) and $h = 0.69\%$ (bottom).

The healing factor obtained in this simplified model is almost identical to the full solution, as shown by the red and green curves of the left panel of Fig. 2 of the main text. This shows that the spinon field fluctuations are utterly irrelevant for the strong healing.

A further fruitful simplification is obtained by setting M_{32} to zero in Eqs. (32). This defines what we called the "minimal model" (MM). In this case, the "strong-correlation sub-block" of δr_i and $\delta\bar{\lambda}_i$ fluctuations decouples and suffers no feed-back from the gap fluctuations. In fact, the MM corresponds to breaking up the solution to the problem into two parts: (i) the spatially fluctuating strong correlation fields r_i and λ_i are first calculated for *fixed, uniform* Δ and χ, and then (ii) the effects of their spatial readjustments are fed back into the gap equation to find $\delta\Delta_i$.

Strikingly, the healing factor in this case is *numerically indistinguishable* from the one obtained from Eqs. (32) (green curve of the left panel of Fig. 2 of the main text). Furthermore, the full, local and non-local PS of gap fluctuations are also captured quite accurately by the MM, as seen in Fig. 2. We conclude that the MM, which incorporates only the effects of strong correlations, is able to describe with very high accuracy the healing process in the d-wave SC state.

The MM also permits us to obtain simple and physically transparent expressions. In particular, it follows immediately that

$$r\delta r\left(\mathbf{k}\right) = \frac{r^2}{\lambda a\left(\mathbf{k}\right) - r^2 M_{33}\left(\mathbf{k}\right)/M_{34}\left(\mathbf{k}\right)}\varepsilon\left(\mathbf{k}\right), \tag{33}$$

where $a\left(\mathbf{k}\right) = 1 - \Gamma_s\left(\mathbf{k}\right)/4$, and we used the Fourier transform of $\mathbf{\Gamma}(s)$, $\Gamma_s\left(\mathbf{k}\right) = 2\left[\cos\left(k_x a\right) + \cos\left(k_y a\right)\right]$. Moreover,

$$\delta\Delta\left(\mathbf{k}\right) = \frac{r^2\left[M_{24}\left(\mathbf{k}\right)M_{33}\left(\mathbf{k}\right) - M_{23}\left(\mathbf{k}\right)M_{34}\left(\mathbf{k}\right)\right]}{M_{22}\left(\mathbf{k}\right)\left[\lambda a\left(\mathbf{k}\right)M_{34}\left(\mathbf{k}\right) - r^2 M_{33}\left(\mathbf{k}\right)\right]}\varepsilon\left(\mathbf{k}\right), \tag{34}$$

$$= \frac{\left[M_{24}\left(\mathbf{k}\right)\frac{M_{33}(\mathbf{k})}{M_{34}(\mathbf{k})} - M_{23}\left(\mathbf{k}\right)\right]}{M_{22}\left(\mathbf{k}\right)}r\delta r\left(\mathbf{k}\right). \tag{35}$$

$$= \chi_{pc}^{MM}\left(\mathbf{k}\right)\delta n\left(\mathbf{k}\right), \tag{36}$$

where we used $n_i = 1 - r_i^2 \Rightarrow \delta n_i = -2r\delta r_i$, and

$$\chi_{pc}^{MM}\left(\mathbf{k}\right) = -\frac{\left[M_{24}\left(\mathbf{k}\right)\frac{M_{33}(\mathbf{k})}{M_{34}(\mathbf{k})} - M_{23}\left(\mathbf{k}\right)\right]}{2M_{22}\left(\mathbf{k}\right)}. \tag{37}$$
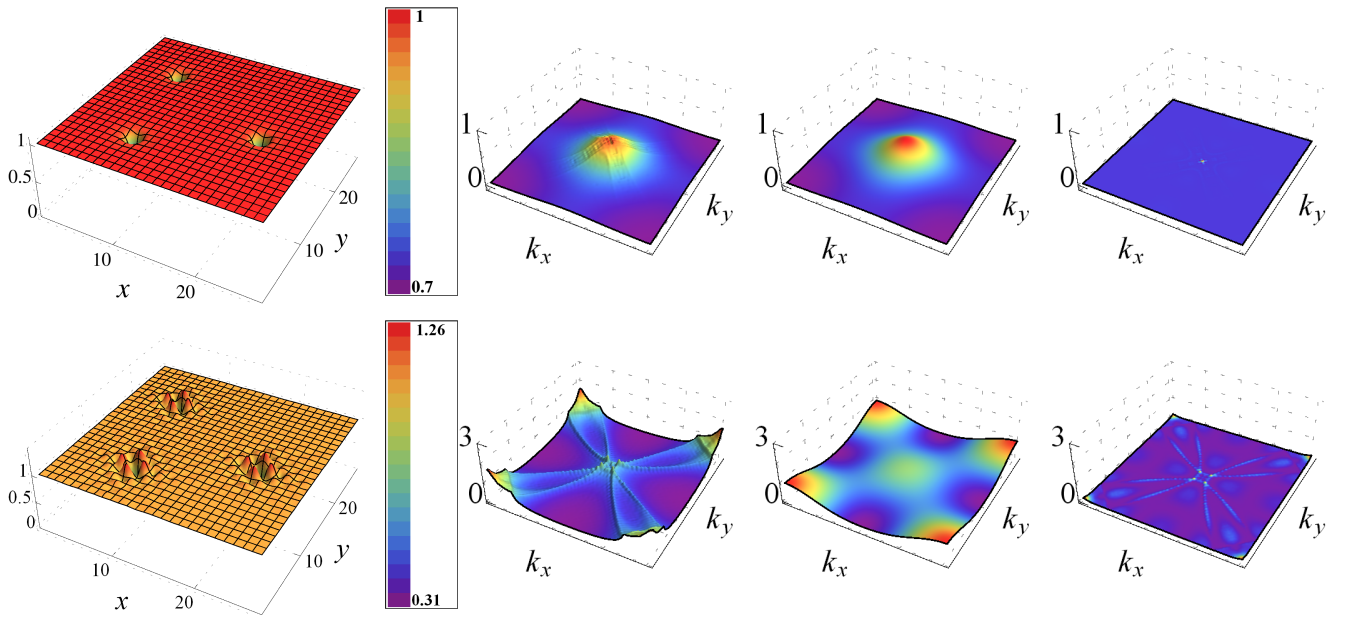
Figure 3: Spatial variations of normalized local density $\frac{\delta n_i}{n_0}$ in the normal state for three impurities (first column) and the corresponding power spectra $N(\mathbf{k})$, $N(\mathbf{k})_{loc}$ and $N(\mathbf{k})_{nonloc}$ (second to fourth columns), in the presence (top) and in the absence (bottom) of strong correlations for $x = 0.2$. The strong suppression of density oscillations by correlations is accompanied by the dominance of the spherically symmetric local power spectrum $[N_{loc}(\mathbf{k})]$ over the anisotropic non-local one $[N_{nonloc}(\mathbf{k})]$.

The local part of the response, which we have shown to be the dominant one, can be studied by looking at the long wavelength limit. As $k \to 0$, $a(\mathbf{k}) \sim k^2/4$ and

$$\delta\Delta_{loc}(\mathbf{k}) \approx -\chi_{pc}^{MM}(\mathbf{k}=0)\frac{8r^2/\lambda}{k^2 + \xi_S^{-2}}\varepsilon(\mathbf{k}), \tag{38}$$

where

$$\frac{1}{\xi_S} = \sqrt{-\frac{4r^2}{\lambda}\frac{M_{33}(\mathbf{k}=0)}{M_{34}(\mathbf{k}=0)}}. \tag{39}$$

Eqs. (37) and (39) give us the expressions for the pair-charge correlation function and the healing length within the MM.

IV. THE NORMAL STATE AND THE "MINIMAL MODEL"

It is instructive to analyze also the behavior of the charge fluctuations in the normal state. This can be achieved by suppressing the second row and column of Eqs. (10) and setting $\Delta(\mathbf{k})$, and thus $g(i\omega_n, \mathbf{k})$, to zero. Even after these simplifications, the full solution is long and cumbersome. However, accurate insight can be gained from a MM of the normal state, in which we also set the $\delta\chi_i$ to zero by hand. As before, the strong-correlation sub-block decouples and Eq. (33) is still valid (albeit with matrix elements calculated in the normal state). The local part of the charge response is given by an expression similar to Eq. (38)

$$\delta n_{loc}(\mathbf{k}) \approx -\frac{8r^2/\lambda}{k^2 + \xi_N^{-2}}\varepsilon(\mathbf{k}), \tag{40}$$

where ξ_N is given by Eq. (39), again with matrix elements calculated in the normal state. The behavior of ξ_N as a function of doping is shown by the green curve of the right panel of Fig. 2 of the main text.

In addition, just like in the Coulomb gas, the density fluctuations also show Friedel-like oscillations coming from the singularity in the response function at $2k_F$. Thus, expanding Eq. (33) in r^2,

$$\delta n_{nonloc}\left(|\mathbf{k}|\approx 2k_F\right)\approx -\frac{2r^2}{\lambda a\left(|\mathbf{k}|\approx 2k_F\right)}\left[1+\frac{r^2 M_{33}\left(|\mathbf{k}|\approx 2k_F\right)/M_{34}\left(|\mathbf{k}|\approx 2k_F\right)}{\lambda a\left(|\mathbf{k}|\approx 2k_F\right)}\right]\varepsilon\left(\mathbf{k}\right).\tag{41}$$

Since

$$M_{34}\left(\mathbf{k}\right) = \mathbf{\Pi}\left(\mathbf{k}\right),\tag{42}$$

$$M_{33}\left(\mathbf{k}\right) = 1+\mathbf{\Pi}^b\left(\mathbf{k}\right),\tag{43}$$

$$\mathbf{\Pi}\left(\mathbf{k}\right) = \frac{1}{V}\sum_{\mathbf{q}}\frac{f\left[\widetilde{h}\left(\mathbf{q}+\mathbf{k}\right)\right]-f\left[\widetilde{h}\left(\mathbf{q}\right)\right]}{\widetilde{h}\left(\mathbf{q}+\mathbf{k}\right)-\widetilde{h}\left(\mathbf{q}\right)},\tag{44}$$

$$\mathbf{\Pi}^b\left(\mathbf{k}\right) = \frac{1}{V}\sum_{\mathbf{q}}\frac{f\left[\widetilde{h}\left(\mathbf{q}+\mathbf{k}\right)\right]-f\left[\widetilde{h}\left(\mathbf{q}\right)\right]}{\widetilde{h}\left(\mathbf{q}+\mathbf{k}\right)-\widetilde{h}\left(\mathbf{q}\right)}\left[h\left(\mathbf{q}+\mathbf{k}\right)+h\left(\mathbf{q}\right)\right],\tag{45}$$

$$h\left(\mathbf{k}\right) = -t\Gamma_s\left(\mathbf{k}\right)-4t'\cos\left(k_x a\right)\cos\left(k_y a\right),\tag{46}$$

the leading divergent behavior is

$$\frac{M_{33}\left(|\mathbf{k}|\approx 2k_F\right)}{M_{34}\left(|\mathbf{k}|\approx 2k_F\right)}\approx\frac{1}{\mathbf{\Pi}\left(|\mathbf{k}|\approx 2k_F\right)}.\tag{47}$$

The two contributions from Eqs. (40) and (41) together give, in real space,

$$\frac{\delta n_i}{n_0} = x\sum_j\left(c_1\frac{e^{-r_{ij}/\xi}}{\xi^{(d-3)/2}(r_{ij})^{(d-1)/2}}+c_2 x\left[\mathbf{\Pi^{-1}}\right]_{ij}\right)\varepsilon_j,\tag{48}$$

where r_{ij} is the distance between sites i and j, and c_1 and c_2 are constants that depend on t,t',J and x.

We stress that in the full solution of the linearized equations in which $\delta\chi_i\neq 0$, the structure of Eq. (33) is still preserved, with the factor M_{33}/M_{34} being replaced by a long combination of several M_{ij} elements, which, however, has a *finite negative* $\mathbf{k}\to 0$ *limit and a singularity at* $2k_F$. Therefore, the results of Eqs. (40), (41) and (48) remain valid in the general case. The spatial charge fluctuations for three impurities and the PS in the normal state in the full solution are shown in Fig. 3 both in the absence and in the presence of strong correlations. Note how the non-local part is down by an additional factor of x as compared to the local part [see Eqs. (41) and (48)].

---

[1] P. Lee, N. Nagaosa, and X. Wen, Rev. Mod. Phys. **78**, 17 (2006).

[2] The usual choice $\widetilde{J}=\frac{1}{4}J$ does not change the analytical results and would give rise to hardly noticeable changes in the numerical plots.